

## Cell response to sol-gel derived titania coatings

D. B. Haddow,<sup>a</sup> J. M. Kelly,<sup>a</sup> P. F. James,<sup>a</sup> R. D. Short,<sup>a</sup> A. M. Scutt,<sup>b</sup> R. Rawsterne<sup>c</sup> and S. Kothari<sup>\*c</sup>

<sup>a</sup>Department of Engineering Materials, University of Sheffield, Mappin Street, Sheffield, UK S1 3JD

<sup>b</sup>Human Metabolism and Clinical Biochemistry, University of Sheffield, Sheffield, UK S10 2RX

<sup>c</sup>Manchester Materials Science Centre, UMIST, Grosvenor Street, Manchester, UK M1 7HS

Received 3rd August 2000, Accepted 12th September 2000

First published as an Advance Article on the web 1st November 2000

Sol-gel derived titania coatings are being developed for use as biomedical coatings. In this study, bone marrow stromal (BMS) cells and ROS osteoblast-like cells have been cultured on sol-gel derived titania coatings and are compared with cultures on glass and tissue culture plastic (TCPS) surfaces. Over 24 h both the BMS and ROS cells attach well to all three substrates. On the titania coatings both cell types spread well, displaying morphologies that conform with those expected of these cells. The ROS cells did not spread well on the glass or TCPS surfaces.

The titania coatings were deposited onto glass by means of an alkoxide sol-gel route and characterised using a number of analytical techniques, including X-ray photoelectron spectroscopy (XPS). The effects of withdrawal rate (in the dipping process) and firing temperature on coating integrity and adherence (to the glass substrate) have been investigated. From this study, parameters have been identified that yield thin, smooth, crack-free titania coatings of homogeneous surface chemistry.

### Introduction

Considerable scientific focus is being given to improving our understanding of material-cell interactions.<sup>1-5</sup> The juxtaposition of synthetic materials with living 'matter' (cells) is becoming increasingly common place in emerging technologies, e.g. implantable biomaterials, tissue engineering, biotechnology, as well as in cell culture experiments. This paper is concerned with the fabrication of titania coatings by an alkoxide sol-gel route, their characterisation by analytical methods and cell (osteoblast) response to these surfaces. This study is relevant to biomaterial (implant) science and cell culture.

Titanium (Ti) and its alloys are amongst the most biocompatible materials and are widely used as dental and orthopaedic implants. When implanted in the body, the surrounding bone forms an intimate contact with the Ti. This close apposition has been termed "osseointegration" by clinicians and has been attributed to the spontaneously-formed oxide layer found on the Ti surface. Despite continued efforts at explaining the processes occurring at the Ti-cell interface, our understanding of this phenomenon remains unclear. It has been postulated, however, that for osseointegration to occur, protein adsorption, cellular adherence, proliferation, differentiation, matrix production and calcification must take place.<sup>6,7</sup> One school of thought attributes the biocompatibility of Ti to the formation of a calcium phosphate layer on the surface of the metal.<sup>8</sup>

The deposition of thin titania films onto a diverse range of substrates may be potentially exploitable in novel implants, or as new surfaces for the culture of particular cell types.<sup>9</sup> In respect of the latter, the majority of commercially available surfaces are plastic (PS or PET) with propriety surface treatments. Our interest is in the fabrication of surfaces on which we can probe bone cell-synthetic material interactions.

A number of techniques are available for the deposition of thin film coatings. These techniques include chemical vapour

deposition (CVD),<sup>10-13</sup> magnetron sputtering/physical vapour deposition (PVD)<sup>14,15</sup> and plasma-based routes (which overlap with CVD, e.g. plasma-assisted CVD).<sup>16</sup> This list is not comprehensive. All of these techniques have been employed in the deposition of titania films or films containing titania and are reviewed by Laube *et al.*<sup>17</sup>

The disadvantage of these techniques is that they require large capital investment, including vacuum systems, electron beam evaporators and/or r.f. heating. In this study, sol-gel has been chosen as the technique for the deposition of titania films. This process was selected on the grounds that little capital equipment is required, except for an electrical motor, magnetic stirrer and chemicals. Possible problems, such as achieving sufficient adherence to the substrate, cracking and surface topography, are envisaged and these are considered later.

The sol-gel process is a low temperature route for the production of inorganic materials.<sup>18</sup> It allows materials to be mixed at a molecular level in a solution, using a solvent. The solvent can then be evaporated off to leave a solid with a high level of fine porosity. During subsequent heat treatment, residual organics are driven off, resulting in the formation of a dense oxide. These techniques may be used to prepare thin coatings on a variety of substrates since the process is independent of substrate shape or size.

There are two main sol-gel routes, the alkoxide and the colloidal routes.<sup>19</sup> The alkoxide route was employed for the synthesis of coatings in this study. Transfer of a thin film of wet gel to a solid-phase substrate was achieved by dip-coating and conversion of a wet gel to a dry one was carried out by a drying phase at ambient temperatures. Finally, this dry gel was converted into densified glass by heat treating the gel at temperatures higher than those used for drying.

Titania films have previously been prepared by the sol-gel route from tetrabutylorthotitanate.<sup>20-22</sup> This precursor was used to produce films on silica. Crystal growth was observed with increasing sintering temperatures. Firing at 500 °C gave anatase, whilst a firing temperature of 1000 °C produced rutile.

XPS was used to examine the chemical composition of two coatings prepared from different precursor/water mixes. Although the firing temperature was not given, it is presumed to have been 500 °C. The Ti 2p core line showed a clear signal at 458.5 eV which was assigned to Ti<sup>4+</sup> and the oxygen, O 1s core line signal at 529.9 eV was assigned to the O<sup>2-</sup> in TiO<sub>2</sub>. Although a signal was seen at higher binding energy in the O 1s core line, this was not commented upon. Sodium (Na 1s) and carbon (C 1s) were also detected.

In a previous study by some of the authors of the current study,<sup>23</sup> sol-gel derived titania films were obtained from Ti tetraisopropoxide. These films were analysed by XPS. Elemental composition was monitored for firing temperatures in the range 100–600 °C (1 h and 3 h). Although, narrow scan spectra for the C 1s and O 1s core levels were reported, these were not peak-fitted, and therefore only a “broad” description of the functional group chemistries of films fired at different temperature was given. No comments were made upon the “bulk” properties of the coatings with firing temperatures.

In this report we concentrate on thin planar films on glass substrates, employing a more comprehensive array of analytical techniques to characterise these materials for porosity, quantitative surface elemental composition and elemental binding state information, crystallinity and surface topography. Comparison is made to the surface chemistry of commercial pure (cp)Ti polished to 0.05 µm. Cell response to sol-gel derived titania, glass and tissue culture plastic (TCPS) is determined by the attachment and spreading of bone marrow stromal cells (BMSC) and ROS (17/2.8) osteoblast-like cells.

## Experimental

### Materials

Plain silicate glass (soda lime) cover slips and microscope slide pieces (Fisons Scientific Equipment, UK) that had been ultrasonically cleaned and washed with distilled water and ethanol were used as substrates. The starting sol was prepared by dissolving Ti tetraisopropoxide (13 ml) in isopropanol (50 ml). The chelating agent, diethanolamine, was added to stabilise the sol. All chemicals were obtained from Aldrich Chemical Co. Ltd., UK.

TCPS (6 well treated tissue culture PS) was obtained from Corning (NY). (cp)Ti samples (>99.6%) were obtained from Titanium International (UK) in the form of a 0.8 mm thick sheet. From this sheet 13 mm discs were stamped. These discs were polished to 0.05 µm, through a series of successive polishes (240 grade Si C paper, 9 µm diamond paste, 1 µm+polishing oil, 1/20 µm+OPS). The quality of surface finish was confirmed by scanning electron microscopy (Philips SEM 505).

### Coating synthesis

The above mixture was sealed from atmospheric moisture and magnetically stirred for 24 h. Gel formation was initiated by the addition of distilled water (0.8 ml) before dipping. Coating was carried out at controlled withdrawal rates, (*U*), using a stepper motor, in a laminar flow cabinet. To determine the optimum rate for the production of crack-free coatings the cover slips were withdrawn at *U*=2.0, 1.0, 0.5 and 0.1 mm s<sup>-1</sup>. The gel forming process was completed by air-drying for 30 min. Densification was achieved by firing over a range of temperatures (100–600 °C) for 3 h in an air furnace. The heating rate was 10 °C min<sup>-1</sup>, unless otherwise stated. The solvent is thus evaporated off to leave a solid coating. Samples were stored in clean glass containers before spectral examination.

### Characterisation of coatings

The optimum *U* for production of crack-free coatings was determined by examining the films under an Olympus BH-MPS optical microscope. Electron microscopy was performed using a Camscan Series 2 and Philips P500 scanning electron microscopes with an accelerating voltage of 20 kV, with magnifications of up to 5000.

AFM was carried out in the tapping-mode using a Dimension<sup>TM</sup> 3000 AFM (Digital Instruments Inc., Santa Barbara, California).

The level of adherence to the underlying substrate was tested by washing weighed samples in hot water (50 °C) (with magnetic stirring) for 12 h. After washing, the films were examined using optical and electron microscopy (Camscan Series 2) and re-weighed to find the % loss in coating mass.

Porosity (*p*) was estimated from the refractive indices of the titania films prepared at the minimum withdrawal speed (*U*=0.1 mm s<sup>-1</sup>). These were measured using an Abbe Refractometer/Hg source. Refractive index was converted to film *p* using the Lorentz-Lorenz equation<sup>24</sup> using the refractive index of anatase (2.65 at 500 nm).<sup>25</sup>

### Coating composition/surface analysis

Samples for XPS analysis were placed directly on aluminium stubs using double-sided adhesive tape. XP spectra were recorded on a VG Scientific spectrometer using Mg-Kα X-rays, an operating source power of 100 W and a take-off angle of 45° with respect to the sample surface, unless otherwise stated. Take-off angles of 20°, 45° and 70° (titania) and 20° and 90° [(cp)Ti] were also used to observe chemical composition at different sampling depths. Survey spectra (0–1100 eV) and spectra of the Ti 2p<sub>3/2</sub>, O 1s and C 1s regions were acquired for each sample using analyser pass energies of 50 and 20 eV, respectively.

The spectra reported in this study were acquired using Spectra 6.0 software (R. Unwin Software, Cheshire, UK) and subsequent processing was carried out with Scienta data processing software (Scienta Instruments, Uppsala, Sweden). The spectrometer was calibrated using the Au 4f<sub>7/2</sub> peak position at 84.00 eV and the separation between the C 1s and F 1s peak positions in a sample of PTFE measured at 397.2 eV, which compares well with the value of 397.19 eV reported by Beamson and Briggs.<sup>26</sup> The measurements reported in Fig. 2 (see later) were made using the VGS 5000 data system with VGS software.

In order to determine surface compositions from XPS data, peak area ratios are converted into atomic percent ratios, using accurate sensitivity factors (sfs). In this study, the sfs of Ward and Wood<sup>27</sup> were employed.

### X-Ray diffraction

XRD was used to obtain data on changes in structure with heat treatment. X-Ray spectra were obtained on a Phillips PW 1710 diffractometer using Co-Kα radiation. Scans were performed at 40 kV and 30 mA with a step size of 0.02° and a speed of 0.02 s<sup>-1</sup> over a 2θ range of 20–65°. Data analyses (background subtraction, smoothing, peak numbering *etc.*) were carried out using Sietronics PW 1710 diffractometer automations software.

### Cell culture

**Preparation of bone marrow stromal cell (BMSC) cultures.** BMSC were obtained from the tibia and femora of 125 g male wistar rats. The bones were excised under aseptic conditions, proximal ends removed and bones placed in microfuge tubes and centrifuged at 2000 rpm for 5 s. The resulting cell clump was dispersed by repeated pipetting and a single cell suspension achieved by forcefully expelling the cells

through a 20 gauge needle. The single cell nature of the suspension was confirmed by microscopic analysis. Secondary culture was established by plating the cells at a density of  $10^7$  cells  $\text{cm}^{-2}$  in DMEM (Dulbecco's modification of Eagle's minimum essential medium) supplemented with 12% FCS, glutamine, sodium pyruvate, sodium bicarbonate and penicillin/streptomycin. Confluent cells were removed using 0.2% trypsin/EDTA and resuspended in 20 ml medium. A single cell suspension was obtained once again by passing the mixture through a 20 gauge needle. Cells were then seeded onto test materials in 24 well plates at a density of  $3 \times 10^4$  cells  $\text{cm}^{-2}$ .

**Preparation of ROS 17/2.8 cells.** ROS 17/2.8 cells (donated by GA Rodan of Merck, Sharp & Dohme, USA) were fast thawed from storage in liquid nitrogen. They were cultured at 37 °C and 5%  $\text{CO}_2$  in Hams F12 nutrient mix (Gibco, UK) supplemented with 10% FCS, glutamine and penicillin/streptomycin. Confluent cells were removed using 0.2% trypsin/EDTA and resuspended in 20 ml medium. A single cell suspension was obtained once again by passing the mixture through a 20 gauge needle. Cells were then passed onto the test materials in 24 well plates at a density of  $3 \times 10^4$  cells  $\text{cm}^{-2}$ .

### Staining and counting

Cells were removed after incubation periods of 3 h and 24 h. They were washed in PBS and fixed in methanol, before staining with methylene blue. Cell numbers were determined by counting under a light microscope in phase contrast (Fig. 5; see later). For each sample, cells were counted for at least 20 fields of view of size 1  $\text{mm}^2$ . Following fixing and staining, samples were placed on microscope slides and optical images obtained using a Leica DM RB fluorescent light microscope.

## Results

### Effect of $U$

The influence of  $U$  on coating thickness and integrity was investigated. Coatings were prepared at four different  $U$  (2.0, 1.0, 0.5 and 0.1  $\text{mm s}^{-1}$ ) and were fired at temperatures in the range of 100–600 °C, the latter being the highest firing temperature used in this study. The effect of  $U$  and firing temperature on coating thickness can be seen in Fig. 1. TEM observation of selected films showed that the observed film thicknesses corresponded closely to those calculated from the coating mass.<sup>28</sup> The thickness of the coatings decreased with increasing temperature for all  $U$ . Thinner coatings were produced at the lowest  $U$ , with the thinnest film (0.029  $\mu\text{m}$ ) being produced at the lowest  $U$  and the highest firing temperature.

Films withdrawn at  $U=0.5$  and 0.1  $\text{mm s}^{-1}$  and fired at temperatures in the range of 100–600 °C were inspected by optical microscopy. Visual observations are summarised in Table 1. All "as withdrawn" films (*i.e.* unfired) were crack-free, irrespective of  $U$ . However, as can be seen from Table 1, at  $U=0.5$   $\text{mm s}^{-1}$ , film cracking becomes more extensive as firing temperature increased (> 300 °C). At greater  $U$ , cracking was

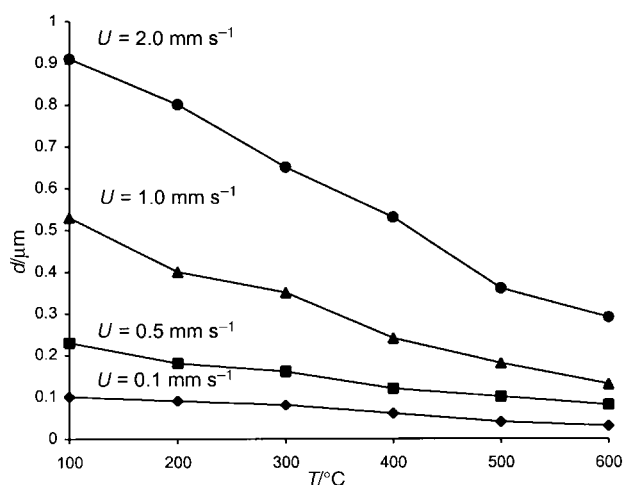


**Fig. 1** Variation in coating thickness with withdrawal speed and temperature.

observed in films fired at > 100 °C. Crack-free and densified coatings were produced at only the lowest dipping speed (0.1  $\text{mm s}^{-1}$ ). For the remainder of this study, all titania samples were fabricated at the lowest  $U$  (0.1  $\text{mm s}^{-1}$ ).

### Adherence

Table 1 also shows the results of the adherence experiment (final column) for coatings obtained for  $U=0.1$   $\text{mm s}^{-1}$ , where the % mass loss in each coating was determined from weighing the samples before and after washing. Below 300 °C substantial mass loss occurred in the coatings typically 50% at 100 °C and 200 °C. At  $U=2.0$   $\text{mm s}^{-1}$ , the mass loss was nearly 100%. Above 300 °C,  $U$  and firing time had no effect on adherence and all the films remained intact. Visual examination (light microscope) revealed that below 300 °C, sections of the films were washed off by warm water.

### Porosity

The porosity in the coatings was determined at several different firing temperatures. At 100 °C, the porosity was between 30–40%, at 300 °C somewhat less than 20% and by 500 °C it was below 15%. Firing at 600 °C did not reduce the porosity any further.

### Coating composition

The elemental compositions of sol-gel films prepared at firing temperatures ranging from 100–600 °C were investigated by XPS, and the quantified results are shown in Fig. 2. This figure gives the elemental compositions of these films (excluding hydrogen) as atom%. The firing time (3 h) was kept constant. By adjusting the heating rate to 1 °C  $\text{min}^{-1}$  up to 600 °C, it was possible to reduce the C content in sol-gel coatings even further, to below 10% ( $7.2\% \pm 1.5\%$  [1sd]).

The peak-fitted Ti 2p<sub>3/2</sub>, O 1s and C 1s core line spectra for a film fired at 600 °C for 3 h are shown in Figs. 3a–c, respectively,

**Table 1** Film appearance as a function of heat treatment and percentage loss in film mass after washing for different withdrawal rates ( $U$ )

| $U=0.5$ $\text{mm s}^{-1}$ |                                     | $U=0.1$ $\text{mm s}^{-1}$ |                        |                          |
|----------------------------|-------------------------------------|----------------------------|------------------------|--------------------------|
| $T/^\circ\text{C}$         | Film appearance                     | $T/^\circ\text{C}$         | Film appearance        | Coating mass loss        |
| 100                        | Virtually crack-free                | 100                        | Smooth crack-free film | Peel-off = 50%           |
| 200                        | Slight cracking                     | 200                        | Smooth crack-free film | Peel-off = 46%           |
| 300                        | Crack network begins to spread      | 300                        | Smooth crack-free film | crack-free film, no loss |
| 400                        | Significant cracking across coating | 400                        | Smooth crack-free film | crack-free film, no loss |
| 500                        | Extensive cracking                  | 500                        | Smooth crack-free film | crack-free film, no loss |
| 600                        | Total film cracking                 | 600                        | Smooth crack-free film | crack-free film, no loss |

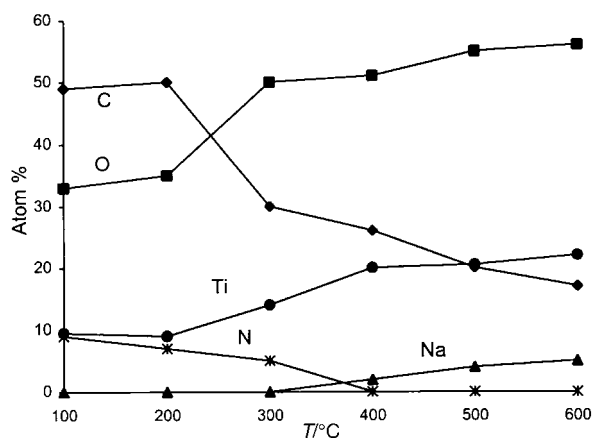


**Fig. 2** Quantified XPS data for sol-gel titania film fired for 3 h over the temperature range 100–600 °C.

with binding energies corrected to hydrocarbon at 285 eV. The position of the Ti 2p<sub>3/2</sub> core line was 458.6 eV, consistent with Ti<sup>4+</sup>. The O 1s has been fitted using three peaks with binding energies of 529.8, 531.8 and 533.1 eV. The 529.8 eV peak corresponds to O<sup>2-</sup> (associated with the Ti<sup>4+</sup>). The two peaks at higher binding energies can not be uniquely assigned. The peak at 531.8 eV may have contributions from C=O (surface contamination)<sup>26</sup> and Ti-OH or surface defects in the TiO<sub>2</sub> oxide layer.<sup>29</sup> The peak at 533.1 eV may have contributions from C-O-C and C-OH (surface contamination)<sup>26</sup> and H<sub>2</sub>O adsorbed at the oxide layer surface.<sup>29</sup> Four peaks have been required to fit the C 1s core line. Hydrocarbon (C-C, C-H) has been set at 285 eV. At 286.4 eV a contribution from C-OH or C-O-C has been fitted and at 288.1 eV a signal for C=O has been included. The relatively high signal at 289.5 eV (O-C=O) is probably added to by overlap with the Na Auger feature.

Depth profiling was undertaken for a film fired at 600 °C (3 h). Three different electron take-off angles were employed, 20°, 45° and 70°. The results in Table 2 indicate that there was little variation in film elemental composition with take-off angles. This result suggests that the C in the film is not a surface contaminant, but is trapped within the film.

All subsequent coatings for biological evaluation were produced at a *U* of 0.1 mm s<sup>-1</sup> and fired at a temperature of 600 °C for 3 h, these being the optimal treatment conditions. One coating from every batch produced was characterised by XPS in order to evaluate reproducibility.

Coatings produced at a *U* of 0.1 mm s<sup>-1</sup> and fired at 600 °C for 3 h were essentially featureless by optical microscopy and SEM. This was confirmed by AFM, samples having a typical root mean square roughness of 4.2 nm.

### X-Ray diffraction (XRD) of fired coatings

XRD patterns were obtained from the sol-gel derived coatings.<sup>30</sup> These showed the coatings to be amorphous up to 400 °C, above which they crystallised to form anatase. A significant orientation along the [101] direction was observed as the degree of crystallisation increased with firing temperature.

**Table 2** XPS determined atomic composition (atom%, excluding H) depth profile for a titania sol-gel film fired at 600 °C for 3 h

| Take-off angles/° | Composition/atom% |      |      |     |
|-------------------|-------------------|------|------|-----|
|                   | C                 | Ti   | O    | Na  |
| 20                | 11.1              | 28.0 | 58.5 | 2.4 |
| 45                | 11.5              | 26.8 | 58.6 | 3.0 |
| 70                | 11.7              | 27.2 | 57.6 | 3.4 |

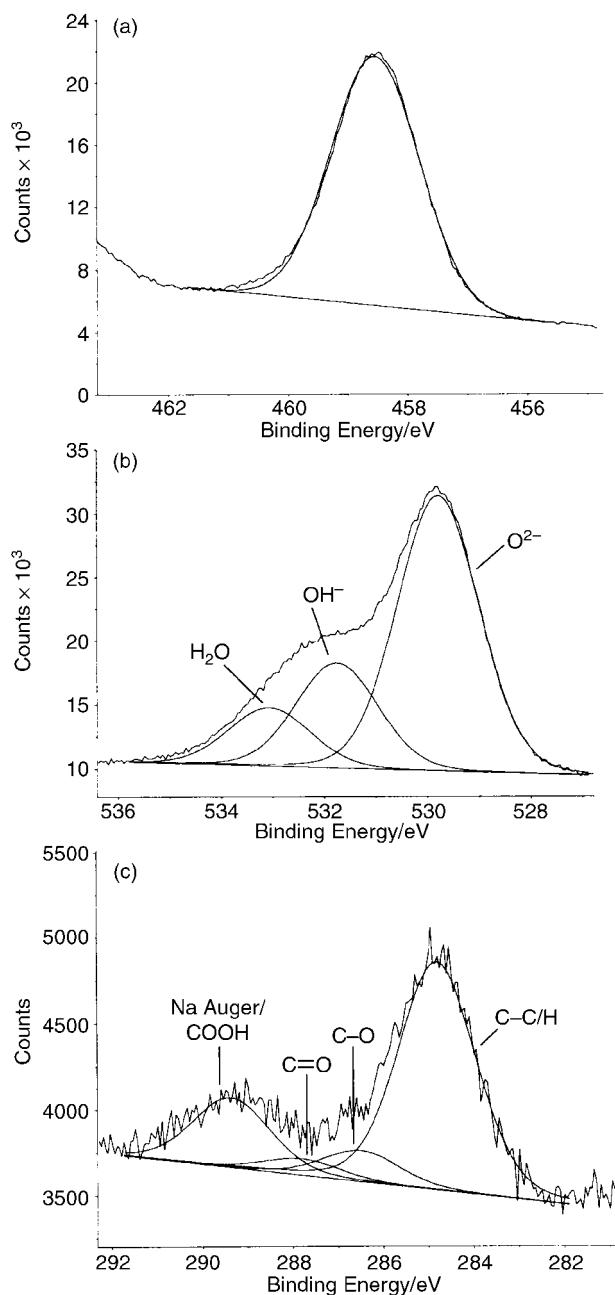


**Fig. 3** XPS core line spectra from a sol-gel titania film fired at 600 °C for 3 h. (a) Ti 2p<sub>3/2</sub>, (b) O 1s, (c) C 1s.

### XPS of (cp)Ti

The surface chemistry of a polished sample of (cp)Ti (0.05 μm) was measured by XPS at 20° and 90° take-off angles. Signals were detected from a number of different core lines, and the respective contributions of elements quantified in Table 3.

The elements detected on the (cp)Ti surface correspond to

**Table 3** XPS determined atomic composition (atom%, excluding H) for 0.05 μm polished titanium at 20° and 90° respectively

| Element | Composition/atom% |      |
|---------|-------------------|------|
|         | 20°               | 90°  |
| C       | 35.8              | 23.9 |
| O       | 43.3              | 50.5 |
| Ti      | 17.8              | 22.6 |
| N       | 2.4               | 2.3  |
| Ca      | 0.6               | 0.3  |
| Na      | 0.1               | 0.4  |

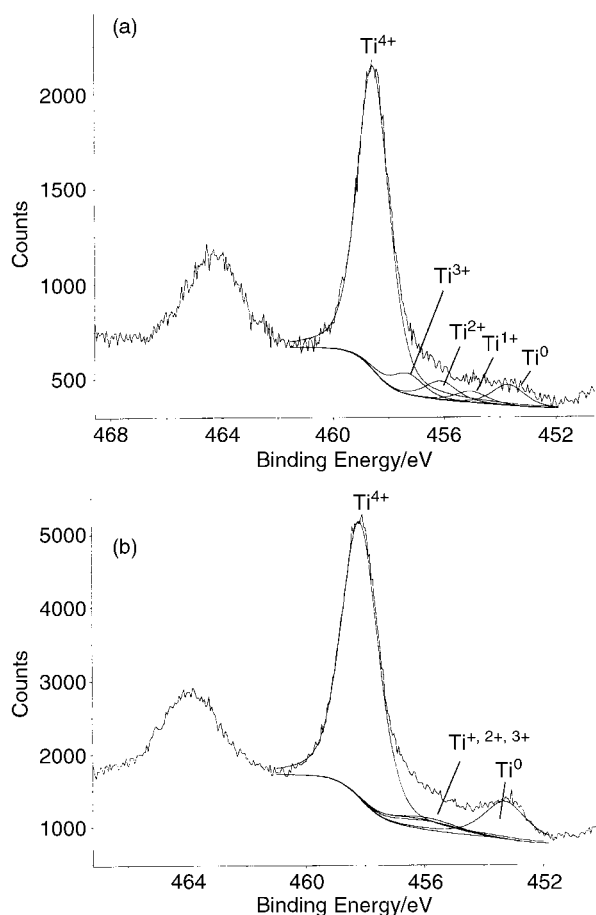


**Fig. 4** Peak-fitted Ti  $2p_{3/2}$  core line spectra of  $0.05 \mu\text{m}$  polished titanium: (a)  $20^\circ$  and (b)  $90^\circ$  take-off angles, respectively.

some of those previously reported by Hernández de Gatica *et al.*<sup>31</sup> and Lausmaa<sup>29</sup> on the surfaces of machined, “as received” and detergent washed Ti-6Al-4V alloys and (cp)Ti.

The data in Table 3 clearly indicate that C is predominantly located at the material’s surface, which contrasts with the sol-gel surface, where C is located throughout the XPS sampling depth.

The Ti and some of the O are “native” to the sample, and it is the chemical states of these elements that are of particular interest. Displayed in Fig. 4 are the peak-fitted Ti  $2p_{3/2}$  core lines recorded at  $20^\circ$  and  $90^\circ$ . Core lines have been fitted using five peaks corresponding (from lowest binding energy upwards) Ti,  $\text{Ti}^{+1}$ ,  $\text{Ti}^{+2}$ ,  $\text{Ti}^{+3}$ ,  $\text{Ti}^{+4}$ .<sup>29–32</sup> The Ti  $2p_{3/2}$  core line spectra were fitted using a Shirley background on the basis that some of the material being sampled was a metal. This is in keeping with the approach by Callen *et al.* in ref. 32 but not that by Callen *et al.* in ref. 33. From Fig. 4 it is evident that more metal is being sampled at  $90^\circ$  than  $20^\circ$ . A higher proportion of the Ti is in the more highly oxidised +4 state as the Ti surface is approached. The O 1s core line spectra were recorded at  $20^\circ$  and  $90^\circ$  (not shown) and peak-fitted in the same manner as the titania ( $600^\circ\text{C}$ , 3 h) film (Fig. 3b). It was observed that as the Ti surface was approached there was a substantially greater contribution from  $\text{OH}^-$  and  $\text{H}_2\text{O}$  to the total O 1s signal.

### Cell culture

The number of BMS and ROS cells attached to sol-gel titania, glass surfaces and TCPS after 3 h and 24 h were assessed by cell counting. The relevant data are shown in Fig. 5. At 3 h, approximately 60% of the ROS cells had attached to the sol-gel titania, whilst  $<50\%$  of the BMS cells had attached. This difference in ROS and BMS cell attachment was significant

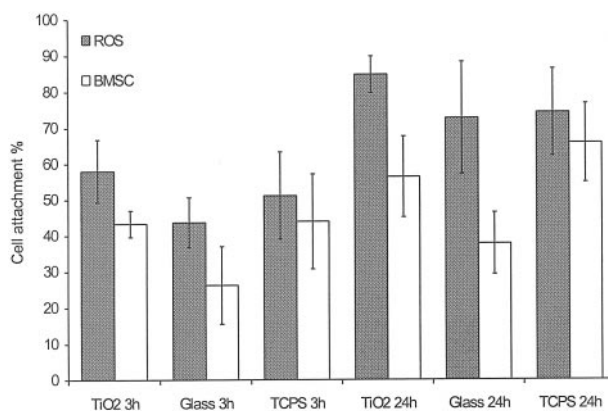


**Fig. 5** Cell attachment of BMS and ROS cells to sol-gel titania, glass and TCPS after 3 h and 24 h of incubation.

( $p < 0.05$ ). On the glass surfaces, the percentage attachments of ROS and BMS cells were approximately 40% and 25%, respectively, but the difference was not significant. It can be seen that at the 3 h time point a greater number of the BMS and ROS cells had attached to the titania surfaces, but the difference was only significant for the BMS cells.

At 24 h, 85% of the ROS cells and 60% of the BMS cells had attached to the sol-gel titania. This assumes no cell division, however, cell division may just be possible at 24 h. On the glass surfaces 70% of the ROS cells and 38% of the BMS cells had attached. On both surfaces more ROS cells attached than did BMS cells and this was significant ( $p < 0.05$ ). At 3 h and 24 h the percentage cell attachment of both ROS and BMS cells on TCPS was very similar to that seen on the titania surfaces.

Although the differences in ROS and BMS percentage cell attachment to titania and glass surfaces at 24 h were not significant, there was a notable difference in the ROS cell spreading. Optical images of the cells at 24 h are presented in Fig. 6. On the sol-gel titania surface, ROS cells have achieved

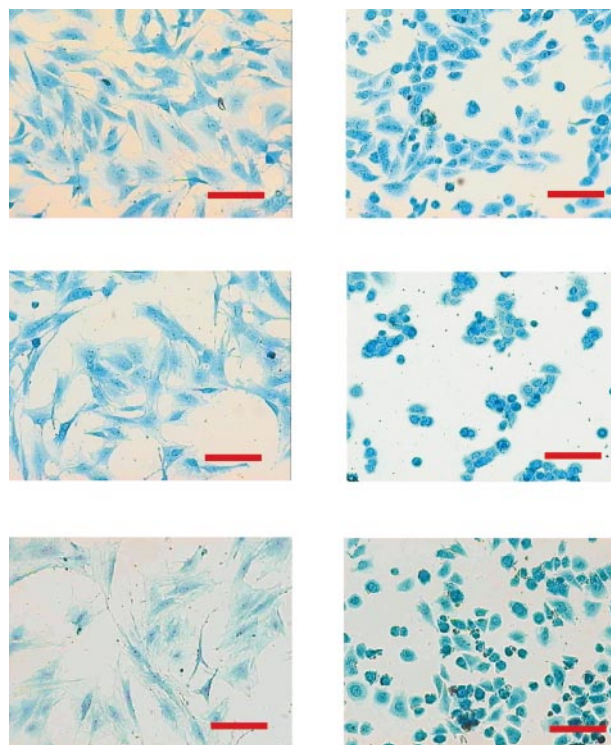


**Fig. 6** Light micrographs of cells incubated for 24 h: (a) BMS cells on sol-gel titania, (b) ROS cells on sol-gel titania, (c) BMS cells on glass, (d) ROS cells on glass, (e) BMS cells on TCPS and (f) ROS cells on TCPS. Cells stained with methylene blue, bar =  $50 \mu\text{m}$ .

their characteristic polygonal morphology (Fig. 6b), but on the glass surface and TCPS the ROS cells remained generally more rounded (Figs. 6d and 6f, respectively). In contrast, the BMS cells have achieved a flattened stellate morphology on all surfaces (Figs. 6a, 6c and 6e).

## Discussion

Determination of the optimum withdrawal speed,  $U$ , for the production of crack-free coatings is crucial to the success of developing coatings for the study of cell cultures. Coating integrity ensures that substrate effects including chemistry and topography do not impinge on cell response to surface coatings.  $U$  has a fundamental effect on coating integrity. Only at a  $U$  of  $0.1 \text{ mm s}^{-1}$  were coatings crack-free across the entire firing range of  $100\text{--}600^\circ\text{C}$  (Table 1). The tendency of thicker coatings to crack upon firing arises from the fact that there is a critical thickness for crack-free coatings, due to contraction effects during the firing/cooling cycle. Thicker films are able to contract in a direction perpendicular to the substrate, and subsequent stress effects lead to the reticular cracking patterns commonly seen in coatings withdrawn at higher rates. At  $600^\circ\text{C}$  the coatings were  $29 \text{ nm}$  ( $290 \text{ \AA}$ ) thick. Coating thickness has been calculated assuming a density  $\rho$  of  $3.84 \text{ g cm}^{-3}$  for anatase.<sup>25</sup> This assumes that  $\rho$  remains constant across all temperatures, but in reality it will increase with firing temperature because heat treatment will induce weight loss ( $\text{H}_2\text{O}$ , 2-propanol) and densification in the films. At higher temperatures (e.g.  $600^\circ\text{C}$ ) the film density will approach that of anatase.

Previous TEM observations of sol-gel titania coatings, which were prepared under these optimum conditions,<sup>28</sup> have shown variations in the coating height of approximately 10% of the coating thickness, i.e.  $3 \text{ nm}$  ( $30 \text{ \AA}$ ). Features of this size are consistent with the rms roughness determined by AFM of  $4.2 \text{ nm}$ . *In vitro* cytocompatibility studies are increasingly concerned with the influence of surface features (roughness and topography) on cell attachment, spreading and proliferation.<sup>34</sup> On  $\text{Ti}_6\text{Al}_4\text{V}$  surfaces it has been shown that cells orientate randomly in the absence of topographical features, and that cell proliferation decreases with (increased) surface roughness.<sup>34</sup> This behaviour has been correlated with a decrease in cell/substrate contact area with increasing roughness. The sol-gel coatings produced in this study were very smooth and this should encourage cell attachment, spreading and proliferation. It is unlikely that features of the order of  $3 \text{ nm}$  would be sufficient to extend any control over cell morphology (e.g. orientation) and migration, which requires features on the micron scale.<sup>35</sup>

Firing temperature also affects coating integrity (Table 1). At temperatures below  $300^\circ\text{C}$  the films were not fully densified and the resulting open pore structure was susceptible to attack by flowing water. Typically, at the optimum  $U$  ( $0.1 \text{ mm s}^{-1}$ ) the % mass loss in film is 50% compared with nearly 100% for a film prepared at  $U=2.0 \text{ mm s}^{-1}$ . As discussed earlier, films withdrawn at higher rates are susceptible to cracking upon drying and these cracks can act as focal points for attack by an aqueous environment and facilitate the peel-off effect seen for films fired at low temperatures ( $100\text{--}200^\circ\text{C}$ ).

XPS analysis of crack-free coatings fired at  $600^\circ\text{C}$  showed that the surface of the material comprised  $\text{Ti}^{4+}$  and O contributions in the form of oxide, hydroxy and physisorbed water. The possible importance of surface hydroxy groups in subsequent apatite formation *in vitro* has been detailed by Li.<sup>36</sup> Depth profiling of the sol-gel titania film revealed that the film chemistry was consistent throughout the sampling depth. In particular carbon-based material (carbon) was incorporated within the film structure rather than merely as a surface contaminant. Pore closure occurs as the films are densified during the drying process, leading to carbon entrapment within

the film. The levels of entrapped carbon can be minimised by employing a low heating rate during the firing process, enabling diffusion of carbon from the open film structure. The chemical nature of the sol-gel films contrasts with that of the (cp)Ti, which also, as expected, exhibits a native oxide layer ( $\text{Ti}^{4+}$ ), but also shows contributions from  $\text{Ti}^{3+}$ ,  $\text{Ti}^{2+}$ ,  $\text{Ti}^+$ , and Ti, as the sampling depth is increased. The reactivity of Ti, resulting in the spontaneous formation of the oxide layer, is sufficient to preclude the possibility that bare metal is exposed at the surface, even on topographically rough specimens. The carbon detected in the (cp)Ti sample is a surface contaminant and its concentration decreases away from the sample surface (Table 3). Perhaps more importantly, the sol-gel titania surfaces exhibit approximately half the carbon contamination ( $<20\%$ ) compared with (cp)Ti ( $\sim 36\%$ ). It is therefore possible to justify that the sol-gel surfaces are chemically 'cleaner' than (cp)Ti.

Sol-gel surfaces are clearly able to replicate the surface chemistry, if not the bulk composition, of (cp)Ti. Although Ti metal is a proven biomaterial, and Ti surfaces promote bone-bonding, it is impractical to use Ti as a culture surface. However, it would be of great advantage to be able to use surfaces which promote bone-bonding, but are easily manipulated and do not require complex processing techniques. It is envisaged that sol-gel titania coatings could form "model" surfaces on which it may be possible to study the cellular mechanisms involved in the *in vivo* mineralisation of Ti implants.

The percentage ROS and BMS cell attachment on titania was comparable to that seen on glass and TCPS (3 h and 24 h). By 24 h both cell types were firmly attached and well spread on the titania surface. TCPS is generally regarded as a "gold standard" for cell culture and the comparable performance of both ROS and BMS cells on this surface and on the sol-gel titania is encouraging. Glass has also been traditionally used as a culture surface and the results presented show this also to be a good surface for cell attachment (BMS and ROS) and spreading (BMS cells only). Elsewhere,<sup>37</sup> we have described the attachment and spreading of ROS and BMS cells to a range of plasma polymerised surfaces at 3 h and 24 h. In comparison with these earlier results, it is clear that all three surfaces investigated in this study are suitable for short-term cell culture.

It is now known that the attachment of cells to the substratum is a complex process involving a number of stages each of which is mediated by specific proteins.<sup>37</sup> The first and perhaps most critical contact between the cell and the substratum is known as "rolling" which is thought to be mediated by the adhesion molecule P-selectin. Disruption of this step leads to a complete lack of adhesion and consequently loss of physiological function. This is then followed by a stage of activation during which the proteins necessary for more firm attachment, principally the integrins, are expressed finally enabling the cells to correctly adhere to the substratum and adopt their correct physiological phenotype. The finding that both ROS and BMS cells attach and spread on the sol-gel surface suggests that the sol-gel surface provides a suitable substrate for the interaction of proteins, either directly or indirectly *via* proteins such as fibronectin present in the culture medium. The cell spreading seen on sol-gel derived titania is of particular importance as this demonstrates that the cells are able to achieve their normal phenotype as seen either *in vivo* or on tissue culture plastic.<sup>38,39</sup> It would also be expected that this would be reflected by an increased ability to synthesise a calcified collagenous matrix, however to demonstrate this is beyond the scope of this particular study.

## Conclusions

Sol-gel titania coatings have been prepared by an alkoxide route. A low withdrawal rate ( $U=0.1 \text{ mm s}^{-1}$ ) and firing

temperature of  $T=600\text{ }^{\circ}\text{C}$  (3 h) produces featureless, thin, crack-free coatings. These coatings are stable under mild ( $50\text{ }^{\circ}\text{C}$ ) aqueous conditions, showing no mass loss or cracking. These coatings show some crystallinity. The coatings are principally  $\text{TiO}_2$ , with a low amount of trapped carbon-based material. At the surface of these coatings there are some Ti-OH functional groups and strongly bound water, which is not removed under UHV conditions (no heating).

Preliminary data from cell attachment and spreading experiments are encouraging. ROS and BMS cells attach well to these sol-gel titania coatings and spread normally. The ease with which these *in vitro* experiments were carried out (*cf.* similar experiments on Ti metal) is encouraging, and leads us to speculate that these sol-gel titania coatings may be very useful as model substrates on which to study bone cell processes, including osseointegration.

## References

- 1 C. A. Scotchford, E. Cooper, S. Downes and G. J. Leggett, *J. Biomed. Mater. Res.*, 1998, **41**, 431.
- 2 D. A. Puleo and R. Bizios, *Bone Miner.*, 1992, **18**, 215.
- 3 J. M. Vasiliev, *J. Cell Suppl.*, 1987, **8**, 1.
- 4 C. R. Howlett, M. D. Evans, W. R. Walsh, G. Johnson and J. G. Steele, *Biomaterials*, 1994, **15**, 213.
- 5 R. Daw, S. Candan, A. J. Devlin, I. M. Brook, S. MacNeil, R. A. Dawson and R. D. Short, *Biomaterials*, 1999, **19**, 1717.
- 6 J. E. Davies, *Anat. Rec.*, 1996, **245**, 426.
- 7 B. D. Boyan, T. W. Hummett, K. Kieswetter, D. Schraub, D. D. Dean and Z. Schwartz, *Cells Mater.*, 1995, **5**, 323.
- 8 T. Hanawa and M. Ota, *Biomaterials*, 1991, **12**, 767.
- 9 Q. Qiu, P. Vincent, B. Lowenberg, M. Sayer and J. E. Davies, *Cells Mater.*, 1993, **3**, 351.
- 10 V. A. C. Haanappel, H. D. van Corbach, R. Hofman, R. W. J. Morssinkhof, T. Franssen and P. J. Gellings, *High Temp. Mater. Processes*, 1996, **15**, 245.
- 11 C. Otterman and K. Bange, *Thin Solid Films*, 1996, **286**, 32.
- 12 K. Segawa, M. Katsuta and F. Kameda, *Catal. Today*, 1996, **29**, 215.
- 13 H. Ha, S. Nam, T. Lim, I. Oh and S. Hong, *J. Membr. Sci.*, 1996, **111**, 81.
- 14 S. Amor, G. Baud, J. Besse and M. Jacquet, *Mater. Sci. Eng.*, 1997, **47**, 110.
- 15 S. BenAmor, G. Baud, J. Besse and M. Jacquet, *Thin Solid Films*, 1997, **293**, 163.
- 16 P. Diaz, M. Edirisinghe and B. Ralph, *Surf. Coat. Technol.*, 1996, **82**, 284.
- 17 M. Laube, W. Wagner, F. Rauch, C. Otterman, K. Bange and H. Niederwald, *Glass Sci. Technol.*, 1994, **67**, 87.
- 18 I. Strawbridge and P. F. James, *J. Non-Cryst. Solids*, 1986, 381.
- 19 P. F. James, *J. Non-Cryst. Solids*, 1988, 93.
- 20 B. Samuneva, V. Kozhukharov, C. Trapalis and R. Kranold, *J. Mater. Sci.*, 1993, **28**, 2353.
- 21 C. Trapalis, V. Kozhukharov, B. Samuneva and P. Stefanov, *J. Mater. Sci.*, 1993, **28**, 1276.
- 22 V. Kozhukharov, C. Trapalis and B. Samuneva, *J. Mater. Sci.*, 1993, **28**, 1283.
- 23 D. B. Haddow, S. Kothari, P. F. James, R. D. Short, P. V. Hatton and R. van Noort, *Biomaterials*, 1996, **17**, 501.
- 24 H. Kragh, *Appl. Opt.*, 1991, **30**, 4688.
- 25 *CRC Handbook of Chemistry and Physics*, ed. David R. Lide, CRC Press, London, UK, 1993.
- 26 G. Beamson and D. Briggs, *High Resolution XPS of Organic Polymers: The Scienta ESCA300 Database*, J. Wiley and Sons, Chichester, 1992.
- 27 R. J. Ward and B. J. Wood, *Surf. Interface Anal.*, 1992, **18**, 679.
- 28 D. B. Haddow, Ph.D. Thesis, *Sol-Gel Titania and Apatite-Like Coatings for Biomedical Applications*, The University of Sheffield, 1997.
- 29 J. Lausmaa, *J. Electron Spectrosc. Relat. Phenom.*, 1996, **81**, 343.
- 30 D. B. Haddow, P. F. James, R. D. Short, S. Kothari, P. V. Hatton and R. van Noort, *Br. Ceram. Proc.*, 1995, 54.
- 31 N. L. Hernández de Gatica, G. L. Jones and J. A. Gardella, *Appl. Surf. Sci.*, 1993, 107.
- 32 B. W. Callen, B. Lowenberg, S. J. Lugowski, R. N. S. Sodhi and J. E. Davies, *J. Biomed. Mater. Res.*, 1995, **29**, 279.
- 33 B. W. Callen, R. N. S. Sodhi and K. Griffiths, *Progr. Surf. Sci.*, 1995, **50**, 269.
- 34 K. Anselme, M. Biggerelle, B. Noel, E. Dufresne, D. Judas, A. Iost and P. Hardouin, *J. Biomed. Mater. Res.*, 2000, **49**, 155.
- 35 A. Curtis and C. Wilkinson, *Biochem. Soc. Symp.*, 1999, **65**, 15.
- 36 P. Li and K. de Groot, *J. Biomed. Mater. Res.*, 1993, **27**, 1495.
- 37 R. Daw, T. O'Leary, J. Kelly, R. D. Short, M. Cambray-Deakin, A. J. Devlin, I. M. Brook, A. Scutt and S. Kothari, *Plasmas Polym.*, 2000, **4**, 113.
- 38 L. Petruzelli, M. Takami and H. D. Humes, *Am. J. Med.*, 1999, **106**, 467.
- 39 J. E. Puzas, *Primer on the Metabolic Bone Diseases and Disorders of Mineral Metabolism*, ed. M. J. Favus, Lippincott-Raven, London, 1996, 3rd edition.